Integrated AVO inversion and seismic attributes for tracing hydrocarbon accumulation in Kafr El-Sheikh Formation, South Batra field, Nile Delta, Egypt: A case study

Mohamed Mostafa GOBASHY[1,*] , Aia Mohamed Fathy DAHROUG[1] ,
Ahmed Hussein ZAKARIA[2], Amr Mohamed SALAHELDIN[3],
Sharafeldin Mahmoud SHARAFELDIN[4]

[1] Geophysics Department, Faculty of Science, Cairo University, Giza, Egypt;
e-mails: gobashy@sci.cu.edu.eg, aiadahroug@sci.cu.edu.eg

[2] Geophysics consultant, Cairo, Egypt

[3] Qantara Petroleum Company, Cairo, Egypt

[4] Geophysics consultant

Abstract: Utilizing advanced seismic techniques for delineating hydrocarbon accumulations in HST (High Stand System Tract) turbidite channel of Kafr El-Sheikh (KS) formation (Pliocene Age) located in the western part of South Batra field (SBF), Nile Delta – Egypt is investigated. 3D seismic data and four well logs helped in studying the properties of the channel. Three wells encountered the central part of the channel and showed thicker reservoir thickness than the fourth well, which encountered the levee. The channel is characterized by high porosity (25–30%) and relatively low water saturation (27–50%). The structural map showed that the channel is dipping towards the NE–SW. AVO analysis, scaled Poisson's ratio, post-stack seismic inversion, and seismic attributes confirmed the presence of Class III gas sand. Variance attribute helped in imaging the channel and faults. Maps generated from spectral decomposition showed that the dominant frequency is around 15 hertz. Results of integrating different techniques were consistent and successfully helped in determining the geometry of the channel, discriminating between different lithologies and fluids, in addition to delineating the sweet spots and recommended locations for drilling.

Key words: AVO inversion, Nile Delta, seismic attributes, variance attribute, spectral decomposition attribute

*corresponding author, e-mail: gobashy@sci.cu.edu.eg

1. Introduction

The Nile Delta basin is the most prolific, prospective gas and condensate province in Egypt. The Nile Delta is the main gas-producing province in the northern part of Egypt with approximately 62 TCF (Trillion Cubic Feet) reserves (*Niazi and Dahi, 2010*) and can be considered the earliest known delta in the world (*Said, 1981*). The present study focuses on the Pliocene section (KS formation) in the western part of SBF in El-Mansoura concession on the eastern side of the Nile Delta area. The study area lies between latitudes 31° 3′ & 31° 9′ N and longitudes 31° 19′ & 31° 22′ E. It is located in the western part of SBF and lies in the central part of El Mansoura Concession northern of El Mansoura City (Fig. 1).
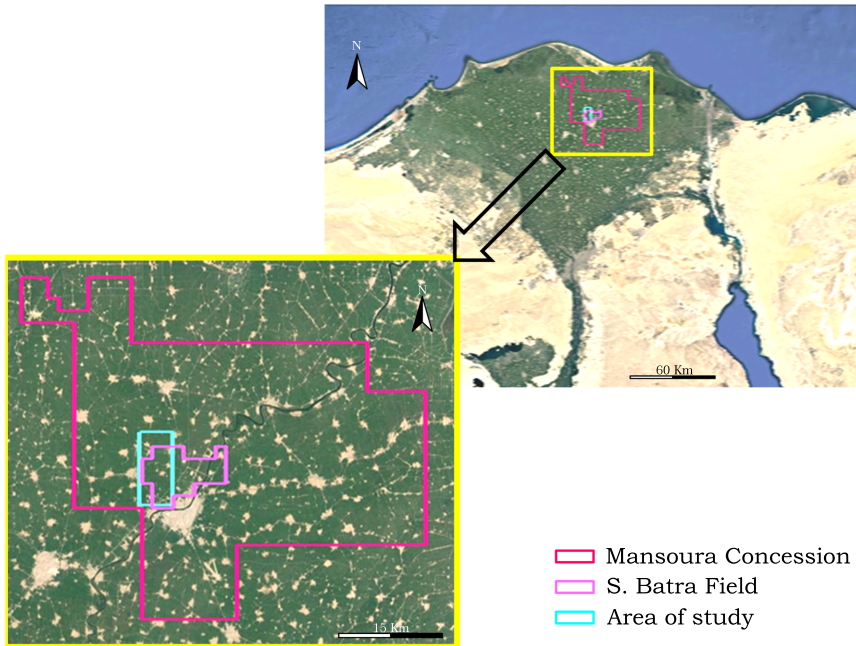

Fig. 1. Geographical location map of the SBF.

The objective of this study is to delineate hydrocarbon accumulations and configure the geometry of the channel/reservoir. This was successfully accomplished by integrating different seismic techniques, including seismic

258

interpretation, seismic inversion, seismic attributes extraction, and AVO analysis.

There are seven wells in the concession (Fig. 2), these wells are (from south to north): South Batra-22, South Batra-17, South Batra-18, South Batra-15A, Mansouria-1, South Batra-8, and Dimayrah-1. All these wells are classified as gas-producing wells; except South Batra-22 is classified as a dry well. This study was based on the data of four wells, which are; South Batra-8, South Batra-15A, South Batra-17, and Mansouria-1 wells.
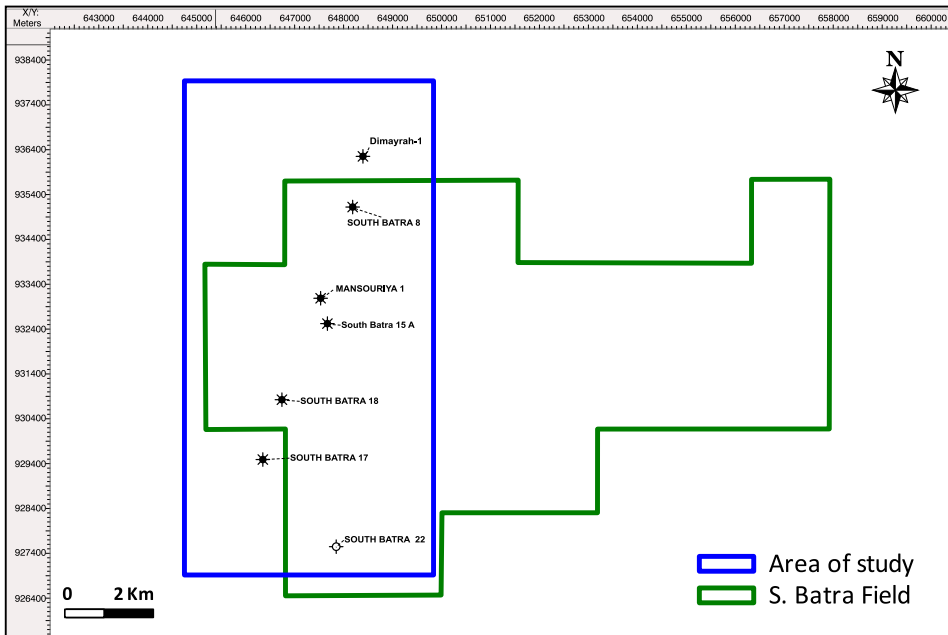

Fig. 2. Location Map of the Area of Study Wells. All these wells are classified as gas-producing wells; except South Batra-22 is classified as a dry well.

Set of logs as Gamma Ray (GR), Sonic, Density, Resistivity, and Check shot helped in studying the petrophysical parameters of the reservoir, in addition to seismic to well tie. Pre-stack seismic data was utilized in the AVO analysis. 3D Post-stack seismic data helped in seismic interpretation for constructing a 3D structural model of the interpreted faults, and horizons, in addition to seismic inversion. The interpretation has been done by using 2D/3D Pak software, which is one module of the Kingdom (SMT)[©]

259

software package, while the AVO Analysis and the seismic inversion have been done by using the Hampson Russell© Software (HRS-9/R2) version.

2. Geological Settings

The stratigraphic sequence of SBF consists of the following Formations from bottom to top: Sidi Salim Formation (Langhian to Tortonian), Qawasim Formation (Early Messinian), Abu Madi Formation (Late Messinian), Kafr El Sheikh Formation (Pliocene), El Wastani Formation (Late Pliocene-Pleistocene), Mit Ghamr Formation (Pleistocene/Recent) (Fig. 3).
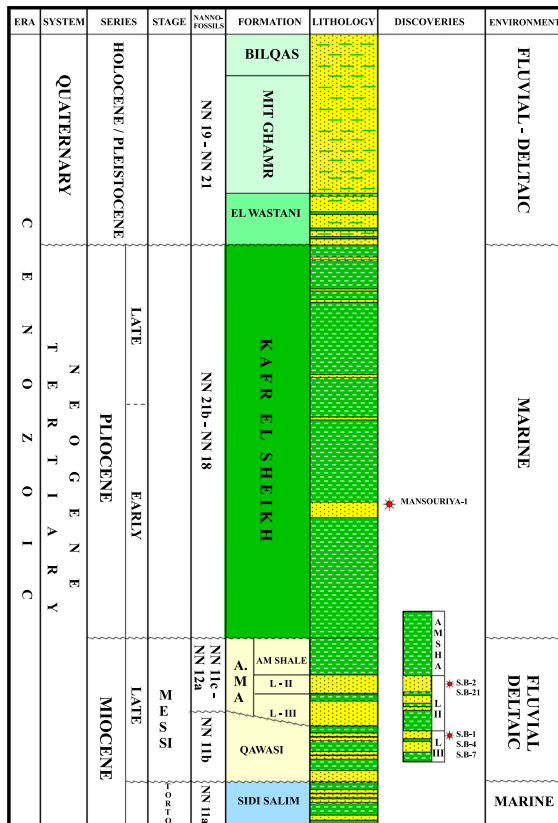

Fig. 3. Generalized lithostratigraphic column of Nile Delta within, showing the stratigraphic sequence of SBF (area of study). The lithology comprises sandstone and shale.

260

Exploration of the KS Formation in the El Mansoura concession is driven
by 3D seismic coverage and interpretation. The prospective areas for the KS
are within the submarine channel systems. Beyond these channels, a mod-
erate risk prospect is proposed. The generation of time slices and horizon
slices revealed 3D geologic patterns that had been impossible to discover
from the geometric interpretation of the wiggle traces in 2D stack sections
(*Avseth et al., 2005*). An arbitrary seismic line (Fig. 4) was selected through
the channel in order to show the mapped regional horizons, in addition to
the encountered wells in the study area. The horizons are Top Wastani
Formation, Top Kafr EL Sheikh Formation, Top Abu Madi Formation, Top
Abu Madi Level II, Top Abu Madi Level III, Top Qawasim Formation, and
Top Sidi Salim Formation.

Stratigraphically, the Pliocene of the Nile Delta unconformably overlies
the Messinian section below it. The Pliocene was marked by a major marine
transgression, which completely overstepped the Messinian incised canyons.
This resulted in the KS marine shales being deposited at the base of the
Pliocene (providing an excellent top seal for the underlying Messinian reser-
voirs) followed by the progradation and deposition of a thick wedge of Kafr
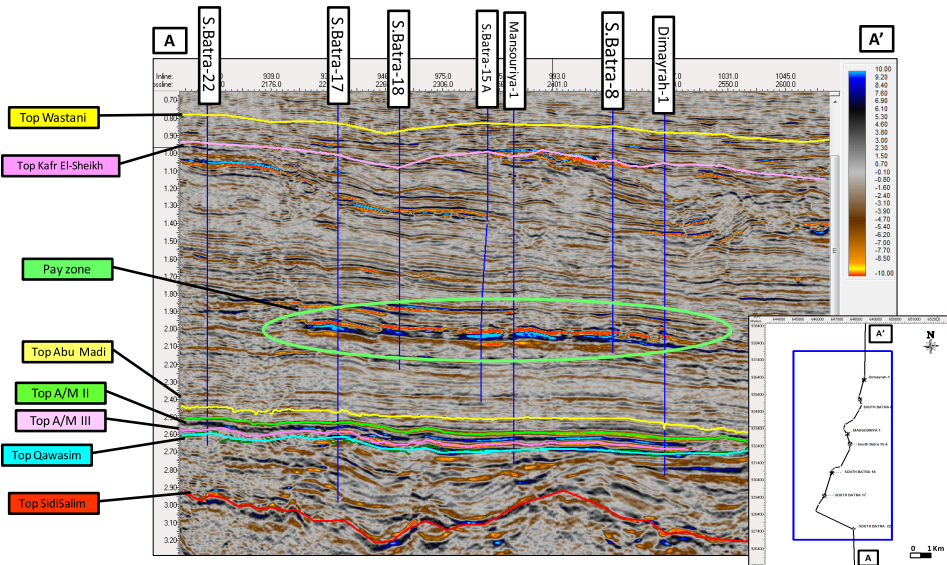

Fig. 4. Arbitrary Seismic line (A–A′) showing the TWT interpreted horizons.

El-Sheikh prodelta muds (*Harms and Wary, 1990*), Channel and turbidite fan sands form the reservoir units of this section, while organic-rich shales provide a biogenic gas source for the Kafr El-Sheikh play. The KS is a proven gas play in the onshore and offshore Nile Delta. A large well database is available for the KS play, including wireline and image logs and core data.

Intra formational KS shale forms the seal for the KS play. As such seal risk for the KS is seen as a low risk throughout the KS of El-Mansoura concession. Hydrocarbons for the KS play are sourced from organic-rich shale units within the Kafr El-Sheikh. These hydrocarbons are generated by biogenic processes and as such the gas encountered in the KS is methane-rich dry gas.

3. Methodology

3.1. Well correlation

Correlating the zone of interest at different well locations will help in understanding the characteristics of the channel. Figure 5 shows stratigraphic correlation profile flatten on top reservoir using the information inferred from available logs (such as; GR, Resistivity, Density, and may be Neutron), especially Sonic and composite logs for S.Batra-17, S.Batra-15A, Mansouria-1 and S.Batra-8 wells.

This correlation assisted in determining the variation of the gross and net thicknesses, and petrophysical parameters of the reservoir such as average porosity and water saturation (Table 1).

Table 1. Gross and net thicknesses, and petrophysical parameters of the reservoir.

Parameters\Wells	S.Batra-17	S.Batra-15A	Mansouria-1	S.Batra-8
GrossThickness(ft)	117	99	58	133
NetThickness(ft)	64	18	13	35
AveragePorosity(%)	25	29	29	30
AverageWaterSaturation(%)	40	30	50	27

Moreover, it turned out that the high reservoir thicknesses at S.Batra-17, S.Batra-15A, and S.Batra-8 wells, because they encountered the central part of the channel, while at Mansouria-1 well the thickness of the reservoir
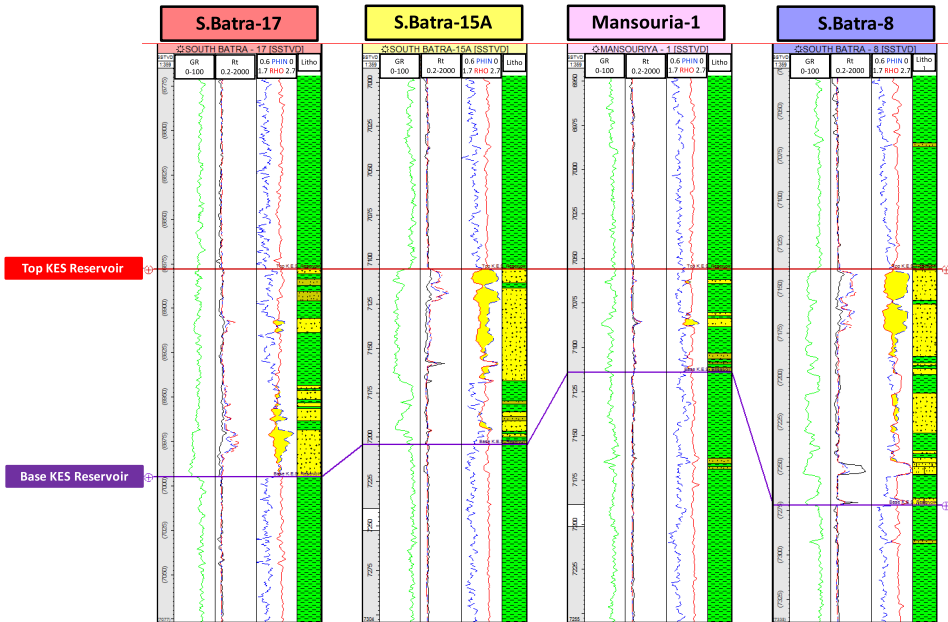
Fig. 5. Well correlation for Kafr El-Sheikh formation at S.Batra-17, S.Batra-15A, Mansouria-1 and S.Batra-8 wells.

is low because it encountered the edge of the channel.

The KS sandstones for these wells are described as loose, colourless, light grey, off white, transparent to translucent, fine to very fine-grained, grading to siltstone size, sub-rounded to sub-angular, moderately sorted, with argillaceous and calcareous cement, and glauconitic in parts. The variation of sand thicknesses and facies within the channel, affect the amplitude and consequently the attribute maps.

3.2. Seismic interpretation

The seismic interpretation is the process, by which information about the subsurface structures of the earth is determined from the seismic sections. This may help in locating new prospects for oil and gas and also may guide the development of an already discovered field. The depth structure contour map is calculated using the Time-Depth relation of the wells to Time-Depth conversion (Fig. 6).
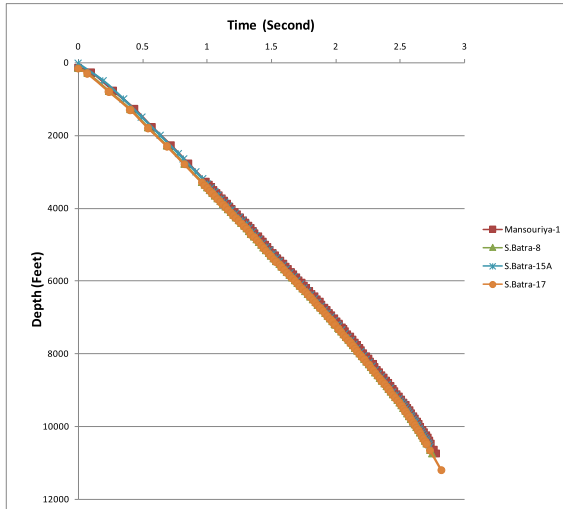
Fig. 6.   Time-Depth relation for S.Batra-8, S.Batra-15A, S.Batra-17 and Mansouria-1 wells.

The depth structure contour map of intra Kafr El Sheikh Sand indicated that the structural dip increases toward NE–SW (Fig. 7), and illustrates that, the depth ranges from 6650 ft to 7300 ft. The large thickness of KS Formation is considered a good sealing for the underlying reservoir as a caprock.

The stacked seismic data volume is commonly used for interpreting geologic structure and seismic attributes. An amplitude extraction map (Fig. 8) was generated in order to identify gas accumulation "bright-spot" and lithological changes. The amplitudes at the well's locations range from −12 to −15.

The amplitude map of KS sand shows the maximum negative true amplitude anomalies that were tested by S.Batra-17, S.Batra-8, S.Batra-18, S.Batra-15A, Mansouria-1, and Dimairah-1 gas discovery wells, while the dimming amplitude areas were tested by S.Batra-22 dry well.

3.3. AVO analysis

Amplitude is affected by variations in rock compositions, stratigraphic conditions, and thicknesses of layers, consequently is considered a Direct Hy-
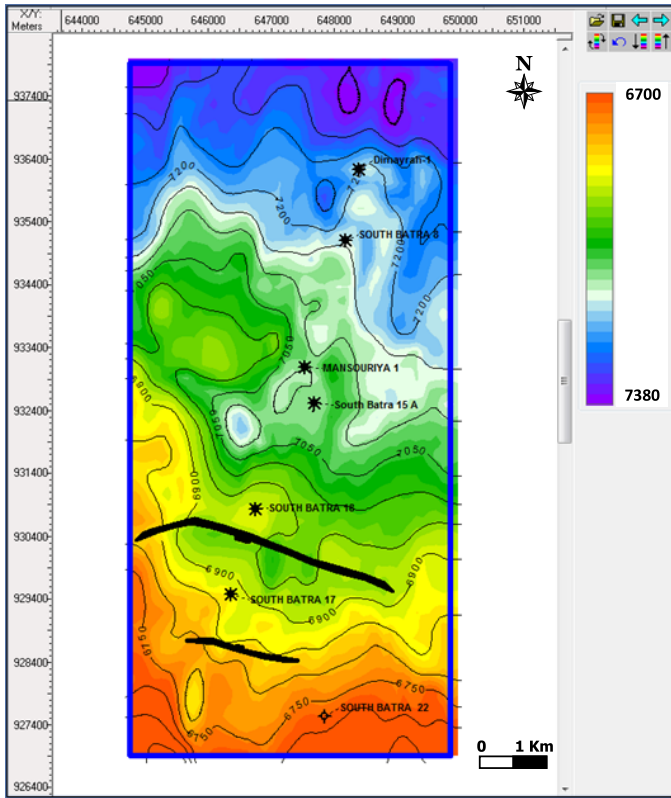
264

Fig. 7. Depth structure contour map for intra KS sand (C.I: 50 ft), where the depth ranges from 6650 ft to 7300 ft.

drocarbon Indicator (DHI). In the case of gas sand saturation, young and shallow sediments are characterized by being unconsolidated and softer (low impedance sand with higher amplitude), while older and deeper sediments are more consolidated and harder (high impedance sand, hence amplitude may be reduced) (*Wren, 1998*). CDP gather at S. Batra-17 well (Fig. 9) shows that the reflector is characterized by high negative amplitude is gradually increasing with offset, therefore it is classified as Class III gas sand.

Comparing extracted amplitude maps (Fig. 10) by using near, med, and far seismic volumes, 0–10, 10–20, and 20–30 degrees respectively, they showed AVO effect due to the presence of gas-bearing sand encountered by the successful wells. On seismic stack data sandstone Class III will be
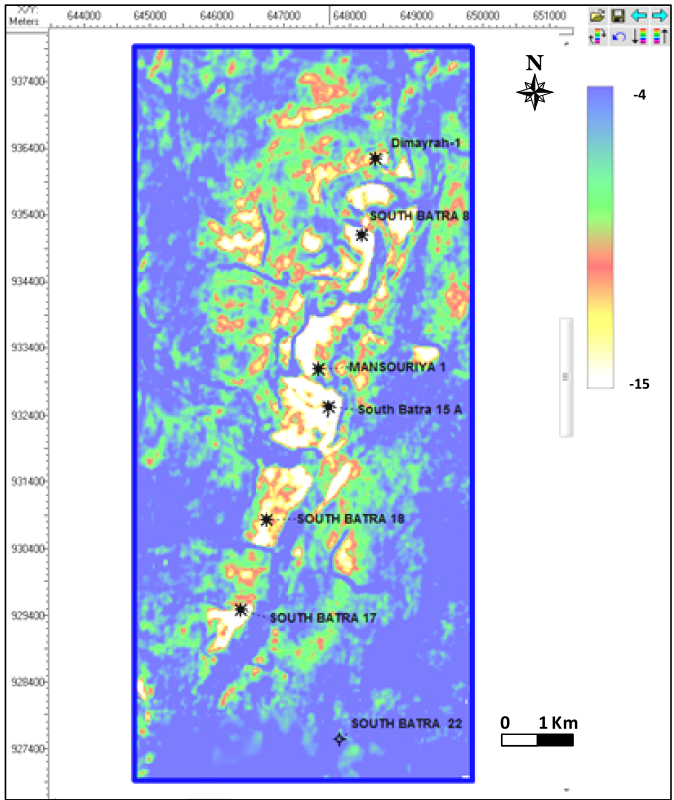
Fig. 8. AVO stack (amplitude) map, which shows the gas accumulations and lithological changes.

characterized by high amplitude anomaly and reflectivity in the whole off-set, so typical bright spots is reflected from class III. Mainly this sandstone is unconsolidated and less compacted sandstone (*NEXT* 4B Module AVO attributes).

3.4. AVO cross plot

AVO interpretation is simplified by cross plotting AVO intercept (A) and gradient (B) (*Young and LoPiccolo, 2004*). The cross plot of intercept and gradient provides a tool for analyzing the AVO responses and determining the appropriate use of intercept and gradient to highlight anomalies (*Castagna and Swan, 1997*) (Fig. 11). *Smith and Gidlow (1987)* stated that
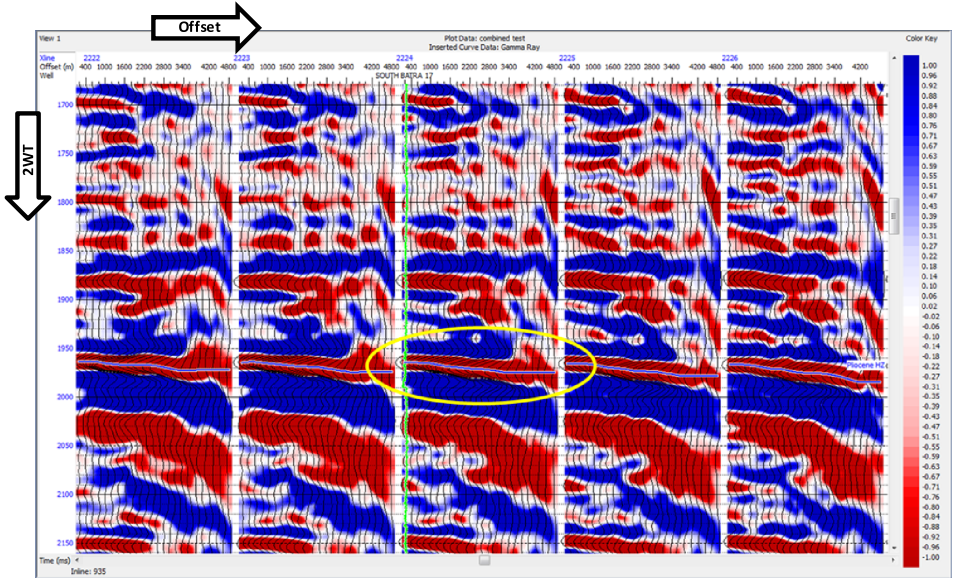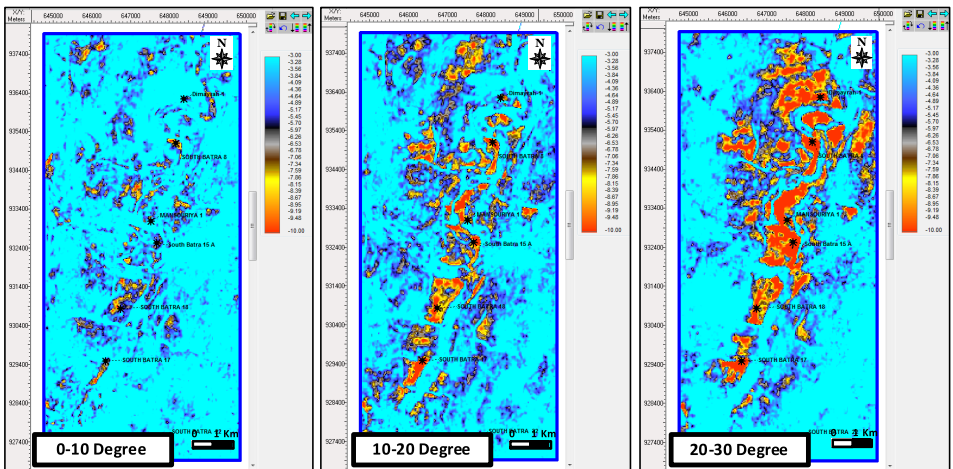
Fig. 9. CDP gather of S.Batra-17 well.

Fig. 10. AVO angles (0–10), (10–20), and (20–30) degree maps.

defining the mud rock line (*Castagna et al., 1985*) in the formula of Shuey indicated a simplified description for the gradient, subsequently, a simple linear combination of both the intercept and gradient yields an optimum
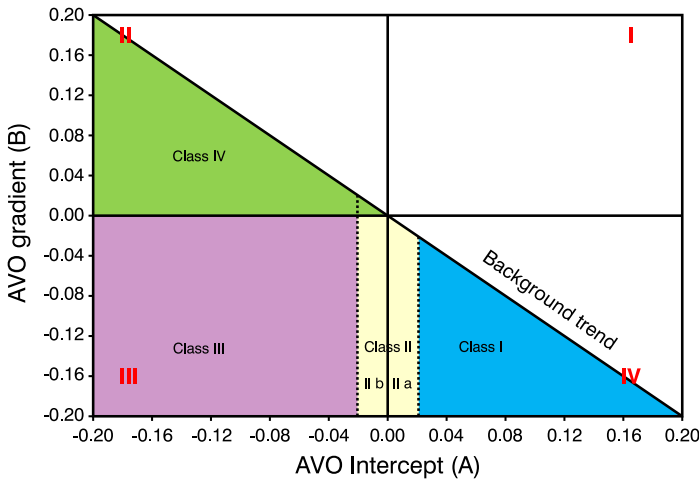
267

Fig. 11. Cross plot of intercept vs gradient (*Castagna and Swan, 1997*).

hydrocarbon indicator, which is called the fluid factor (*Cambois, 1998*).

The P-wave and S-wave velocities ratio is around two, brine filled sands and shales are aligned along a negative trend on cross plotting the intercept versus gradient. This trend is often called the fluid or wet line. Hydrocarbon anomalies are usually aligned away from this trend. *Verm and Hilterman (1994)* reported that the different classes of AVO anomalies (*Rutherford and Williams, 1989; Castagna and Swan, 1997*) will be mapped in various locations on the cross-plots of intercept versus gradient (*Cambois, 1998*). Reflectors of different impedances and polarities will align in different zones of an intercept/gradient cross plot (*Russell, 2003*). The AVO classes fall in particular parts of the cross plot and anomalies can be discriminated either on the basis of zones or as a result of linear combinations of the intercept and gradient (*Castagna et al., 1998*). Cross-plotting Intercept versus Gradient helps in separating lithologies with different fluid densities from the background trend (*Hampson et al., 2004*). The degree of shift will be controlled by the stiffness of the rock. Intercept versus Gradient cross plot confirmed the presence of gas sand; where the background trend is marked by grey colour, while gas sand is marked by red colour and brine sand in blue (Fig. 12).

The presence of Class III gas sand has been confirmed in the study area. Figure 13 shows seismic lines at different well locations by using intercept
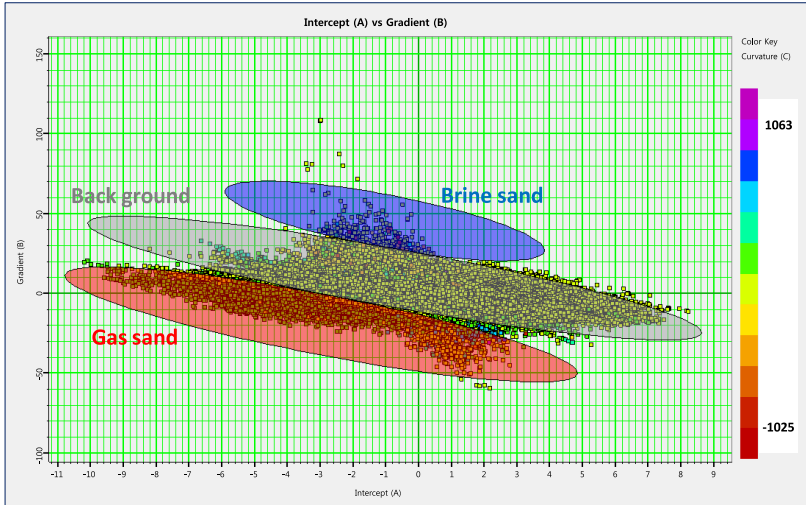
Fig. 12. Cross plot for intercept vs gradient over the area of study in S.Batra Field.
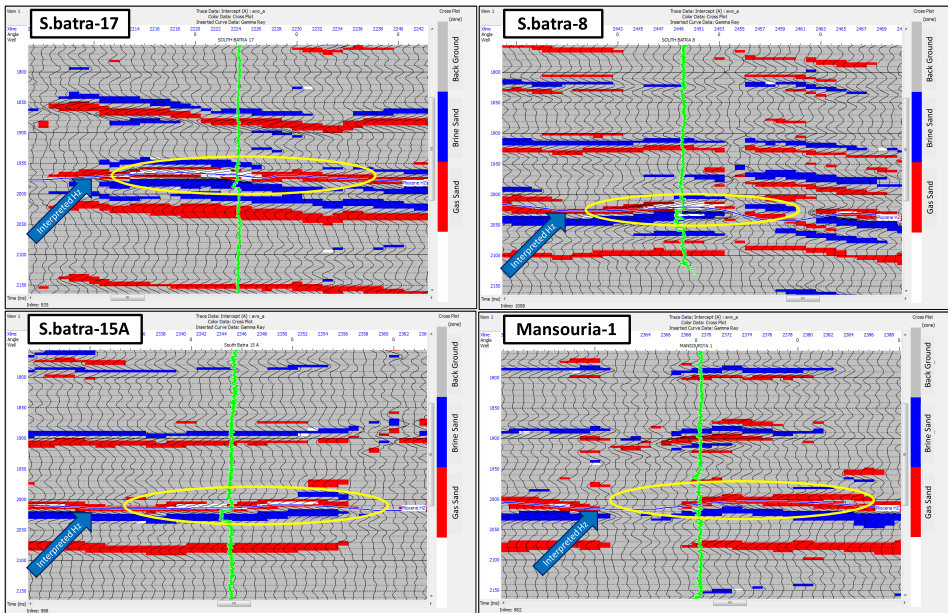

Fig. 13. The gas sand, brine sand, and the background for S.Batra-17, S.Batra-8, S.Batra-15A, and Mansouria-1 wells. By using Intercept volume, while the colour code is by the cross plot data and gamma-ray log demonstrated for calibration.

volume, gas accumulations were indicated. These anomalies are marked within the seismic lines and calibrated with the well logs.

3.5. Intercept and gradient

Rutherford and Williams (1989) stated that there is a linear relationship between the amplitude and sine squared by the angle of incidence (*Shuey, 1985*). The intercept is the amplitude at zero offset/angle, and the gradient is, the slope or function of compressional and shear wave velocities and reflection coefficients, in addition to density contrast and these are useful in locating gas reservoirs. The intercept and gradient are related to the elastic properties of the ground (*Cambois, 1998*). In Hampson Russell© software, the calculation of intercept and gradient volumes from an input pre-stack dataset is simple. Velocity data was provided from S.Batra-17 well as a velocity control. Figure 14 illustrates the AVO response derived from the intercept and gradient volumes. AVO anomaly was successfully indicated by using intercept volume and the product of intercept and gradient as the colour code. AVO anomaly was calibrated by gamma-ray log and top of the pay zone.
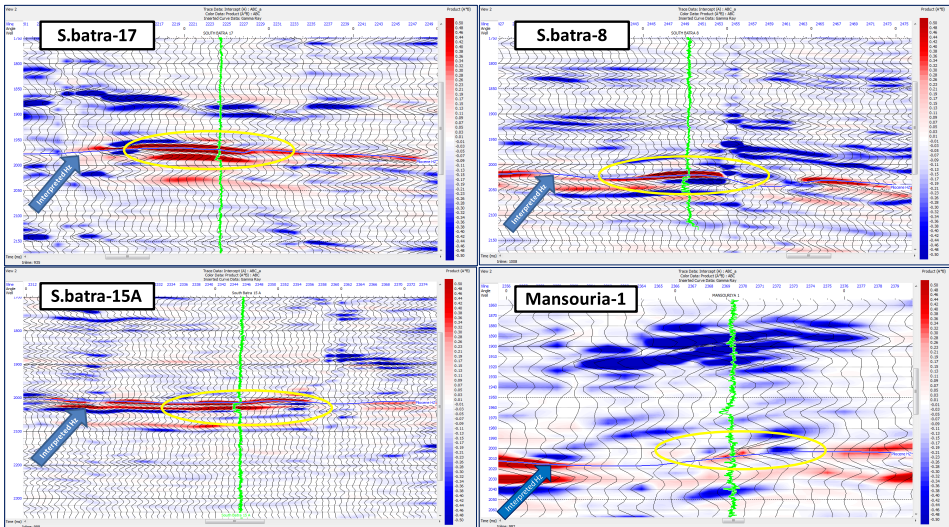

Fig. 14. AVO anomaly at S.Batra-17, S.Batra-8, S. Batra-15A, and Mansouria-1 wells, by using Intercept volume, while the colour code is the multiplication of Intercept and Gradient, and gamma-ray log demonstrated for calibration.

3.6. Poisson's ratio change

The amplitude variation with offset is also affected by Poisson's Ratio ($\sigma = [0.5*(vp/vs)^2 - 1]/[(vp/vs)^2 - 1]$), which is directly related to the ratio of P-wave to S-wave velocity. The equations, which are used to estimate the variations of the amplitude as a function of offset, are reliant on density, P-wave velocity, and Poisson's ratio (*NEXT*; Module 4B attributes AVO). Scaled Poisson's ratio is another attribute, which can be utilized to delineate AVO anomaly. Poisson's ratio is the ratio of deformation of a certain rock in different directions. Figure 15, Seismic lines across the wells by using intercept volume, while the colour code is scaled Poisson's ratio, showed consistency with the previous volume and confirmed the presence of gas accumulations.
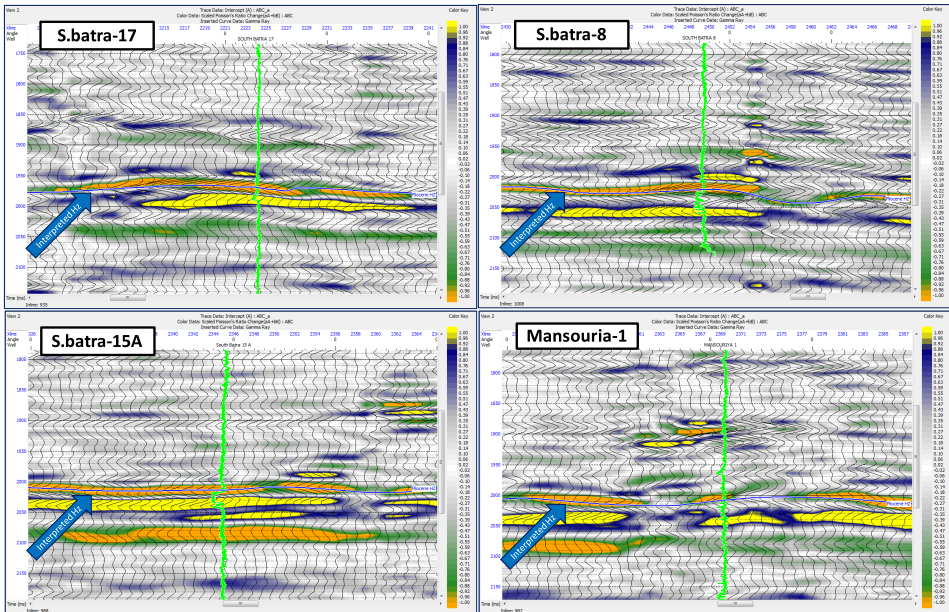

Fig. 15. Change in Poisson's Ratio indicates AVO anomaly for S.Batra-17, S.Batra-8, S.Batra-15A, and Mansouria-1 wells, while the colour code is by scaled Poisson's ratio, and gamma-ray log demonstrated for calibration.

3.7. Post-stack seismic inversion

Three physical parameters of seismic data are fundamental to seismic inter-

pretation: density, P-wave velocity, and S- wave velocity. Densities and P-wave velocities are usually available from well logs and/or core. By correlating these seismically derived properties with values measured in the borehole, interpreters may be able to extend well information throughout the entire seismic volume. This process, called seismic inversion for reservoir characterization, can help fill gaps in our knowledge of formation properties between wells (*Barclay et al., 2008*). Seismic inversion is the process of converting the interface property (i.e. a reflection) to a rock property known as impedance, in order to create absolute acoustic impedance from post-stack seismic data. Within the inverted dataset, the amplitudes are now describing the absolute impedance, which reflects the internal rock properties, such as lithology type, porosity or the fluid type in the rocks (brine or hydrocarbons). The inverted data is ideal for stratigraphic interpretation and reservoir characterization. Seismic inversion is undertaken to complement conventional deconvolution processing (Fig. 16).
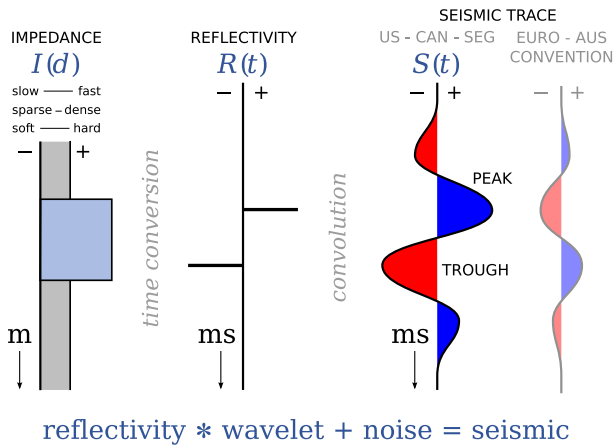

Fig. 16. Showing the convolution/deconvolution process (`https://subsurfwiki.org/wiki/Convolutional_model`).

The acoustic impedance indicates the softness and hardness of lithology. Low acoustic impedance indicates soft lithology, while high acoustic impedance indicates hard one. Arbitrary seismic line A–A′ by using inverted seismic volume across all the wells (Fig. 17), showed that the wells have encountered low impedance lithology (resembled in green colour) due to the presence of Class III gas sand.
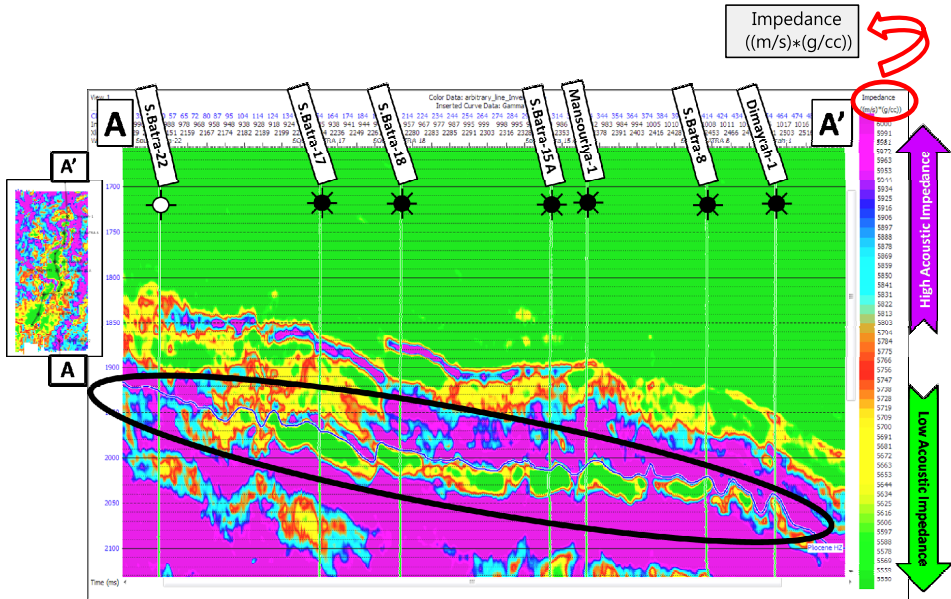
Fig. 17. Arbitrary seismic line A–A′ passing through the wells in the inverted model.

3.8. Variance attribute

Variance attribute (geometric attribute example), which is an edge method to measure traces adjacent or the similarity of waveforms over given lateral and/or vertical windows. Therefore, it can image the discontinuity of seismic data related to fault or stratigraphy. Variance attribute is a very effective tool for delineating and mapping faults and channel edges (*Pigott et al., 2013*) and is also used to display directly the major fault zones, fractures, unconformities, and the major sequence boundaries. Variance attribute map (Fig. 18) was successfully generated, in order to mark the channel edges. The values range from −0.2 to 0.2.

3.9. Spectral decomposition attribute

The purpose of the spectral decomposition is to see the seismic response at different discrete frequency intervals, as higher frequencies image thinner beds, while lower frequencies image thicker beds (*Van Dyke, 2010*). The Spectral Decomposition decomposes trace data into frequency bands. This
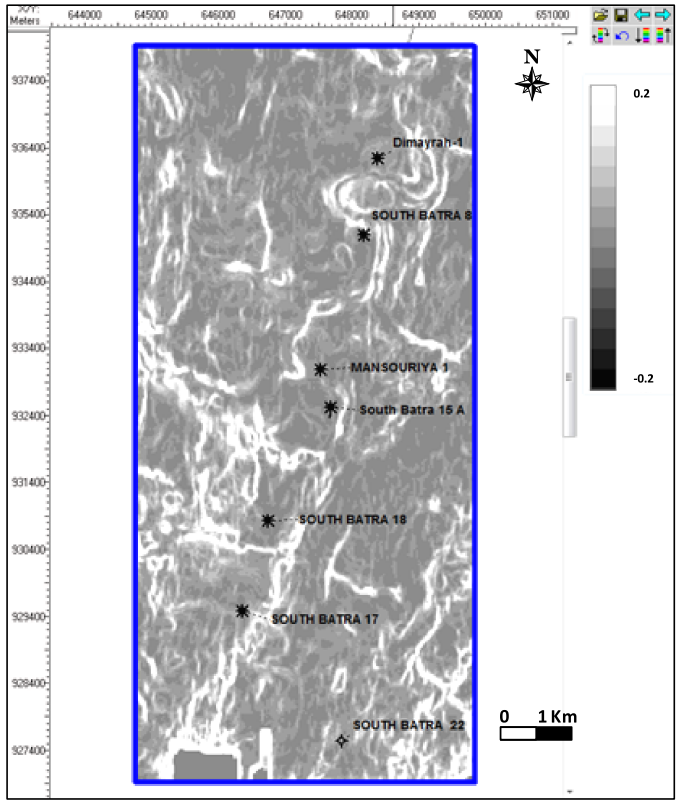
Fig. 18. Variance attribute map, showing the discontinuity due to faults and stratigraphy within the study area. The values ranges from −0.2 to 0.2.

attribute is based on the fact that the seismic data responds differently with each frequency (higher frequency, shorter wavelength, detecting thin channel). In the seismic processing the data spectrum was whitened. Spectral components are affected by different thicknesses and infills, therefore results different spectral responses (*Del Moro, 2012*).

At a specific frequency band, geological features will be observed and highlighted due to tuning effects, etc. This means that for example instead of looking at one phase volume for a cube of stacked data, interpreters are able to view several of them and see if any single one shows a structure or geomorphological information better (*Subrahmanyam and Rao, 2008*). This attribute is very useful to solve the problems of thin-bed sand layers. In

general, thinner beds will be better displayed with higher frequency components and thicker beds with lower frequency. Spectral decomposition maps were generated over the study area from 5–45 Hz (Fig. 19).
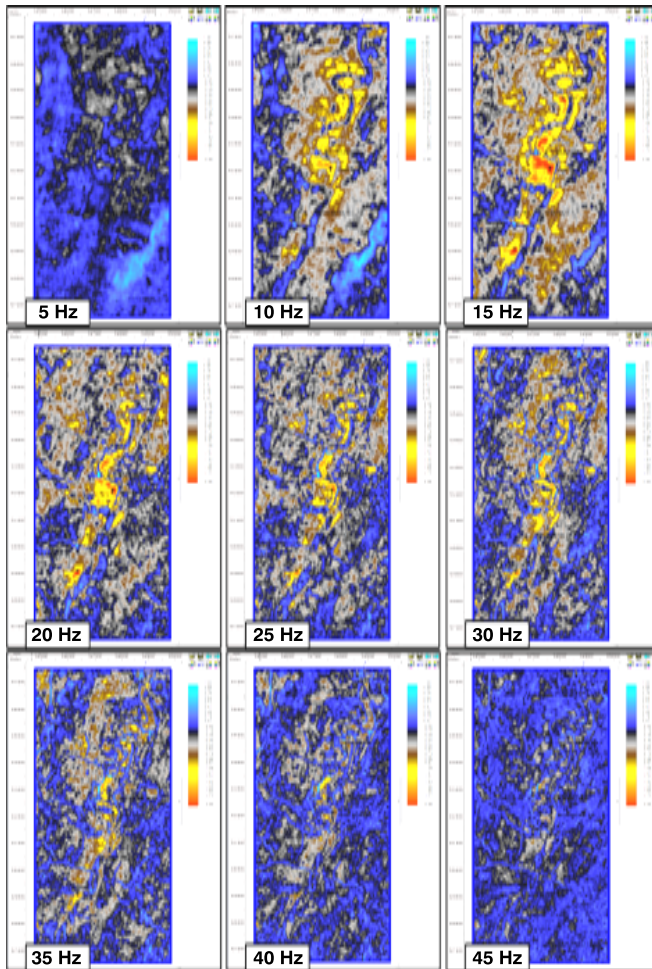

Fig. 19. Spectral decomposition attribute maps from 5 Hz to 45 Hz.

On the other hand, investigating the frequency spectrum of the seismic data of S.Batra Field showed that the dominant frequency is around 13 Hz (Fig. 20).
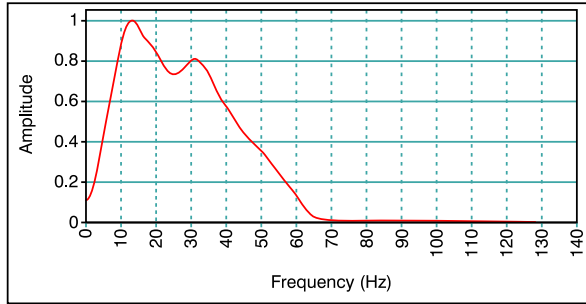
275

Fig. 20. The amplitude–frequency spectrum curve of S.Batra field.

4. Results

Integrating different techniques always provide more details and help in understanding the study area. This has been successfully accomplished in SBF channel. All the wells in the study area were classified as gas wells, except for one well. The well logs showed that the channel is characterized by good net thickness, high average porosity, and low water saturation. The depth of intra KS formation sand ranges from 6650 ft to 7300 ft and is dipping towards NE–SW. An amplitude extraction map was generated and showed the maximum negative amplitude within the study area. CDP gather at S.Batra-17 well and angle stacks volumes proved the presence of Class III gas sand. The results were consistent with Seismic inversion, which helped in detailed interpretation of the channel and confirmed that gas sand in the study area is characterized by a low impedance. Cross-plotting Intercept versus Gradient helped in separating lithologies with different fluid densities from the background trend, therefore hydrocarbon anomalies were aligned away from this trend. Both Intercept and scaled Poisson's ratio showed AVO anomaly and were calibrated with the GR log. A variance attribute map was successfully generated, in order to mark the channel edges. A spectral decomposition map of 15 Hz could provide full details of the channel this is because the dominant frequency is nearly 13 Hz.

5. Discussion

The wells which encountered the central part of the channel showed that it is characterized by high reservoir thickness, while the well which encoun-

tered the levee is characterized by small thickness. Bright-spot resulted on the amplitude extracted map due to the presence from Class III gas sand, which was confirmed by AVO effect from both CDP gather at S.Batra-17, attributes extracted from near, med, far angle stacked volumes. Seismic inversion helped in determining the distribution and extensions of low impedance gas sands in the study area. Intercept and gradient cross plotting and scaled Poisson's ratio could successfully discriminate between different lithologies and different fluids. The maps generated from the amplitude extraction, variance, and spectral decomposition were consistent and showed the details of the meandering channel of KS (Fig. 21).
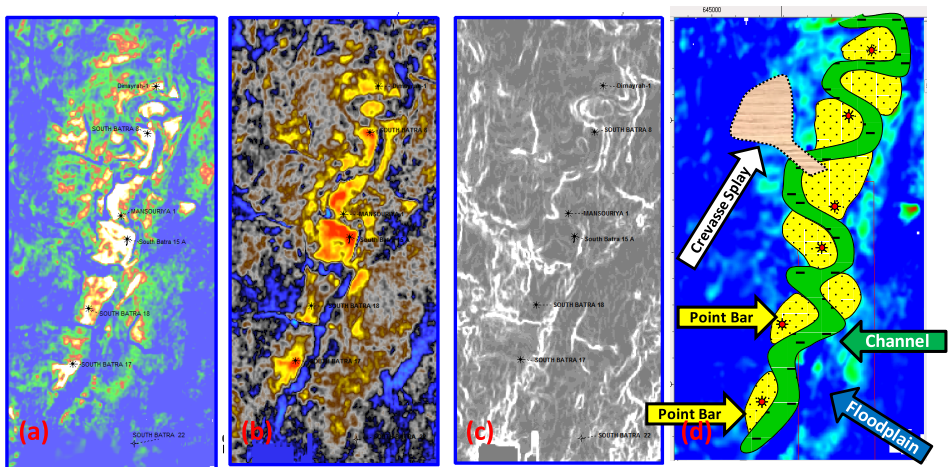

Fig. 21. Channel pattern from different attributes: (a) amplitude extracted map; (b) spectral decomposition 15 Hz; (c) variance map; (d) schematic map of the channel.

6. Summary and conclusion

Different seismic techniques were integrated to trace and determine gas accumulations in HST (High Stand System Tract) turbidite channel of KS formation in SBF, which is located in El-Mansoura concession, Nile Delta, Egypt. In SBF, hydrocarbon is being produced from three main reservoir levels, which are KS formation (Pliocene Age), Abu Madi level II (Messinian Age), and Abu Madi level III (Messinian Age). This study focused on the pay zone intra KS Formation (Pliocene age). 3D seismic data and well logs helped in studying the geometry and properties of the channel. Prestack

and post-stack seismic data were available, in addition to data of four gas-producing wells (S.Batra-17, S.Batra-8, S.Batra-15A, Mansouria-1). The well logs showed that the channel is characterized by a net thickness of 64–13 ft, average porosity 25–30%, and average water saturation of 27–50%. The structural map showed that the channel is dipping towards NE–SW. AVO analysis confirmed the presence of Class III gas sand in the study area. This was proved by gas-producing wells (S.Batra-17, S.Batra-18, S.Batra-15A, Mansouria-1, S.Batra-8, and Dimairah-1), which were clear on the amplitude extracted map, except for S.Batra-22 well, because it is a dry well. Seismic inversion helped in stratigraphic interpretation and delineating low impedance zones. Seismic attributes are very important in order to extract more information from the seismic data. Variance provided information on the stratigraphic edges of the channel, in addition to the faults, while special decomposition showed optimum results of the channel at 15 Hz. All the utilized techniques yielded consistent results and showed that the study area is characterized by Class III gas sand. The generated maps can be successfully used to delineate the sweet spots and recommended locations to be drilled.

References

Avseth P., Mukerji T., Mavko G., 2005: Quantitative Seismic Interpretation: Applying Rock Physics Tools to Reduce Interpretation Risk. Cambridge University Press, 359 p.

Barclay F., Bruun A., Rasmussen K. B., Alfaro J. C., Cooke A., Cooke D., Salter D., Godfrey R., Lowden D., McHugo S., Özdemir H., Pickering S., Pineda F. G., Herwanger J., Volterrani S., Murineddu A., Rasmussen A., Roberts R., 2008: Seismic inversion: Reading between the lines. Oilfield Rev., **20**, 1, 42–63.

Cambois G., 1998: AVO attributes and noise: Pitfalls of crossplotting. SEG Technical Program Expanded Abstracts, 244–247, `doi: 10.1190/1.1820390`.

Castagna J. P., Swan H. W., Foster D. J., 1998: Framework for AVO gradient and intercept interpretation. Geophysics, **63**, 3, 948–956, `doi: 10.1190/1.1444406`.

Castagna J. P., Swan H. W., 1997: Principles of AVO crossplotting. Lead. Edge, **16**, 4, 337–344, `doi: 10.1190/1.1437626`.

Castagna J. P., Batzle M. L., Eastwood R. L., 1985: Relationships between compressional-wave and shear-wave velocities in clastic silicate rocks. Geophysics, **50**, 4, 571–581, `doi: 10.1190/1.1441933`.

Del Moro Y., 2012: An integrated seismic, geologic and petrophysical approach to characterize the Red Fork incise valley fill system in the Anadarko Basin, Oklahoma. M.Sc. Thesis, University of Oklahoma, USA, 121 p.

Hampson D., Russell B., Cardamone M., 2004: Uncertainty in AVO – How can we measure it? Recorder, **29**, 3, 5–11.

Harms J. C., Wary J. L., 1990: Nile Delta (chapter 17). In: Said R. (Ed.): The geology of Egypt. Rotterdam, Netherlands, A. A. Balkema Publishers, 734 p.

Niazi M., Dahi M., 2010: Unexplored giant sandstone features in ultra-deep water, West Mediterranean, Egypt. E.G.P.C, Egypt.

NEXT: Network of Excellence in Training, Module 4B Attributes AVO.

Pigott J. D., Kang M.-H., Han H.-C., 2013: First-order seismic attributes for clasticseismic facies interpretation: Examples from the East China Sea. J. Asian Earth Sci., **66**, 34–54, `doi: 10.1016/j.jseaes.2012.11.043`.

Russell B., 2003: AVO seismic technology. Petroleum Technology Transfer Council (PTTC), Eastern Gulf region PTTC workshop.

Rutherford S. R., Williams R. H., 1989: Amplitude-versus-offset variations in gas sands. Geophysics, **54**, 6, 680–688, `doi: 10.1190/1.1442696`.

Said R., 1981: The geology and evolution of the River Nile. Springer, New York, N.Y., 151 p.

Shuey R. T., 1985: A simplification of the Zeoppritz equations. Geophysics, **50**, 4, 609–614, `doi: 10.1190/1.1441936`.

Smith G. C., Gidlow P. M., 1987: Weighted stacking for rock property estimation and detection of gas. Geophys. Prospect., **35**, 9, 993–1014, `doi: 10.1111/j.1365-2478.19 87.tb00856.x`.

Subrahmanyam D., Rao P. H., 2008: Seismic Attributes – A Review. Hyderabad International Conference and Exposition on Petroleum Geology, 398–403.

Van Dyke S. K., 2010: Spectral Decomposition: A Powerful tool for the seismic interpreter. International basic and applied research journal, Houston, TX 77024, online, accessed on 14/1/2017, `https://www.scribd.com/document/481126554/Spectral-Decomposition-Houston-paper-doc`.

Verm R. W., Hilterman F. J., 1994: Lithologic color-coded sections by AVO crossplots. 64th Annual International Meeting, Society of Exploration Geophysicists Expanded Abstracts, 1092–1095.

Wren E., 1998: AVO: A direct hydrocarbon indicator: Earth Resources Exploration. EREX, 1–236.

Young R. A., LoPiccolo R. D., 2004: Conforming and non-conforming sands – an organizing framework for seismic rock properties: Gulf Coast Association of Geological Societies Transactions, **54**, 767–773.